Arab J Sci Eng (2016) 41:2011–2021
DOI 10.1007/s13369-016-2061-2

RESEARCH ARTICLE - MECHANICAL ENGINEERING

Multiple Quality Characteristics Prediction and Parameter Optimization in Small-Scale Resistance Spot Welding

Xiaodong Wan[1] · **Yuanxun Wang**[1,2] · **Dawei Zhao**[1,2]

Received: 1 June 2015 / Accepted: 24 January 2016 / Published online: 18 February 2016

Abstract This study focuses on prediction and optimization of multiple quality characteristics in small-scale resistance spot welding of titanium alloy. Grey relational analysis was first conducted to roughly estimate the optimum welding parameters combination. Multiple regression analysis was then implemented for a local parameter optimization. Optimum welding parameters were determined by desirability function and multi-objective genetic algorithm approach separately. A back propagation neural network model was also performed to simulate relationship between welding parameters and single output of the first principal component. Performance of the particle swarm optimization was better than genetic algorithm in obtaining optimum welding parameters. The neural network-based model was very effective in global optimization. A good agreement could be found between experimental results and predicted weld quality characteristics. Weld quality could be found significantly improved with the proposed methods.

Keywords Small-scale resistance spot welding · Multi-objective optimization · Principal component analysis · Grey relational analysis · Multiple regression analysis · Neural network

✉ Xiaodong Wan
wanxiaodong@hust.edu.cn

[1] Department of Mechanics, Huazhong University of Science and Technology, Wuhan 430074, China

[2] Hubei Key Laboratory for Engineering Structural Analysis and Safety Assessment, Luoyu Road 1037, Wuhan 430074, China

1 Introduction

Resistance spot welding has been widely applied as a successful manufacturing process. Extensive investigations have been concentrated on traditional "large-scale" resistance spot welding process (LSRSW). With the rapid development of miniaturized devices and components fabrication, small-scale resistance spot welding (SSRSW, $t \leqslant 0.5$ mm) is in great demand. Materials to be welded in SSRSW are generally nonferrous metal, and welding parameters like the electrode force should be set at a much smaller level compared with LSRSW. Recommendations for welding lobe in engineering practice on SSRSW are limited. Simply scaling down welding parameters from LSRSW to SSRSW may lead to expulsion, electrode sticking and non-repeatable welding. Quality management in SSRSW is a critical problem to be investigated.

Titanium alloy is considered as one of the best engineering materials due to the outstanding properties like low density, high specific strength and excellent corrosion resistance. However, special attentions should be paid in welding of titanium alloy. Titanium alloy is reactive to nitrogen and oxygen in the molten state [1]. Kahraman [2] found that atmospheric gases could be isolated effectively in resistance spot welding of pure titanium through electrode pressure implementation. Wan et al. [3] monitored the weld quality in SSRSW of titanium alloy using dynamic resistance and principal component analysis (PCA). An online and real-time quality monitoring system could be developed fundamentally. Limited researches have been conducted on weld quality optimization in SSRSW of titanium alloy by now.

Nugget diameter or failure load is generally adopted as the single quality indicator in LSRSW. Optimum welding parameters combination could be obtained by analyzing the signal-to-noise ratio in Taguchi experimental design. Ely and

Zhou [4] showed that nugget size in SSRSW was about one-third of the electrode diameter. The nugget diameter variation in SSRSW is not that significant compared with LSRSW, and weld quality estimation accuracy is reduced just by considering the nugget diameter. Multiple responses consideration is helpful in obtaining a stable composite weld quality.

Multiple quality characteristics of welding process could be converted into one composite index. Multi-objective optimization is then transformed into optimization of the multi-performance index. This approach is easy to implement in practice. The objective function could be represented by an overall grey relational grade [5,6], overall desirability function [7], principal component [8,9] or multi-signal-to-noise ratio [10].

Kesharwani et al. [5] demonstrated an effective Taguchi method-based grey relational analysis (GRA) on optimizing multiple weld quality characteristics in tailored friction stir butt welding. The desirability function approach for multi-objective optimization is generally in combination with regression analysis [7]. Taguchi-based principal component analysis is also a commonly used method for multi-objective optimization. The multi-performance index could be determined by scores of principal components [8,9]. Muhammad et al. [10] presented the multi-objective Taguchi method to simultaneously optimize nugget diameter and heat-affected zone width in resistance spot welding process. Multi-signal-to-noise ratio was used as the multi-performance index to be optimized.

In the above-mentioned methods, difficulties are existed in objectively selecting weighting coefficients for multi-performance index calculation. At present, artificial intelligence-based methods are drawing more and more attentions. Easiness, effectiveness and simultaneous prediction of multiple quality characteristics are the main advantages. There is no need to convert multiple responses into a single objective function. In general, a statistical model is first developed to establish the relationship between welding inputs and outputs. Multi-objective optimization could then be realized by searching the Pareto front [11,12].

The quality characteristics variation in SSRSW is much smaller than that in LSRSW. Validation of multi-performance index and intelligence-based multi-objective optimization methods is still remain to be discussed. In this study, the titanium alloy SSRSW is conducted and optimum welding parameters combination is established. Multiple quality characteristics are considered for a reliable parameter optimization. Different multi-objective optimization methods are developed and compared with each other. GRA is first conducted to establish a rough estimation of optimum welding parameters. Multiple regression analysis is then implemented to determine local optimum parameters. A back propagation neural network model (BPNN) is also applied to search the global optimum welding parameters combination directly.

2 Methodologies

2.1 Principal Component Analysis (PCA)

The PCA is an effective tool for dimension reduction without much information loss. Each principal component is a linear combination of original multiple responses. All principal components are orthogonal to each other. The procedure could be illustrated as follows:

Step 1: Normalization of original responses array.

Response normalization equation is defined as $\boldsymbol{X}^*$:

$$x_i^*(j) = \frac{x_i(j) - x_i(j)^-}{x_i(j)^+ - x_i(j)^-} \tag{1}$$

where $x_i(j)^+$ is the maximum value in sequence $x_i(j)$, $x_i(j)^-$ is the minimum value in sequence $x_i(j)$.

The original quality characteristics array is represented by $\boldsymbol{X}$:

$$\boldsymbol{X} = \begin{pmatrix} x_1(1) & x_2(1) & \ldots\ldots & x_m(1) \\ x_1(2) & x_2(2) & \ldots\ldots & x_m(2) \\ \vdots & \vdots & \vdots\ \vdots & \vdots \\ x_1(n) & x_2(n) & \ldots\ldots & x_m(n) \end{pmatrix}$$

where m is the quality characteristics number, n is the number of experiment.

Step 2: Calculation of correlation coefficient array $\boldsymbol{R}$.

$$r_{st} = \frac{\mathrm{cov}(x_s^*(j), x_t^*(j))}{\sigma_{x_s^*(j)} \times \sigma_{x_t^*(j)}} \tag{2}$$

where $\mathrm{cov}(x_s^*(j), x_t^*(j))$ is the covariance of sequences $x_s^*(j)$ and $x_t^*(j)$. $\sigma_{x_i^*(j)}$ is the standard deviation of sequence $x_i^*(j)$. Eigenvalues and corresponding eigenvectors could be derived from $\boldsymbol{R}$.

Step 3: Calculation of principal component scores.

$$pc_k(j) = \sum_{i=1}^{m} x_i^*(j) \times v_k(i) \tag{3}$$

where $pc_k(j)$ is the jth component of kth principal component, $v_k(i)$ is the ith component of kth eigenvector.

2.2 Grey Relational Analysis (GRA)

The grey system theory was first proposed by Deng [13]. The grey system-based GRA is useful in solving complicated interrelationships among multiple responses. A sequence of grey relational grade could be obtained to evaluate original multiple quality characteristics. Steps in performing GRA are as follows:

Step 1: Normalization of original responses array.

Table 1 The chemical composition of TC2 titanium alloy, wt%

Alloying elements			Impurities (not higher than)					
Al	Mn	Ti	Fe	C	N	H	O	Others
3.5∼5.0	0.8∼2.0	Bal.	0.30	0.10	0.05	0.012	0.15	0.40

This step is called the grey relational generation, which is the same as that in PCA. A referential series of $\boldsymbol{X}_0^*$ with ideal value of each column is also proposed:

$$\boldsymbol{X}_0^* = \left(x_1^*(0)\ x_2^*(0)\ \ldots\ldots\ x_m^*(0)\right)$$

Step 2: Calculation of the grey relational coefficient ξ.

$$\xi_i(j) = \frac{\Delta\min + \zeta\Delta\max}{\Delta_i(j) + \zeta\Delta\max} \tag{4}$$

where $\Delta_i(j) = \left| x_i^*(0) - x_i^*(j) \right|$, $\Delta\min = \min_i \min_j (\Delta_i(j))$, $\Delta\max = \max_i \max_j (\Delta_i(j))$, ζ is the distinguishing coefficient: $\zeta \in [0, 1]$.

Step 3: Calculation of the grey relational grade γ.

$$\gamma_j = \sum_{i=1}^{m} \omega_i \times \xi_i(j) \tag{5}$$

where ω_i is the weight of each quality characteristic and $\sum_{i=1}^{m} \omega_i = 1$. In this study, ω_i is determined from the PCA.

3 Experimental Procedure

The base material is TC2 titanium alloy with a thickness of 0.4 mm. TC2 is an important titanium alloy used in industries. Chemical composition of TC2 is listed in Table 1. Dimensions of spot-welded specimens are given in Fig. 1. Before welding, TC2 sheets were first polished and then etched with a mixed solution of nitric acid, hydrofluoric acid and water for several minutes. Specimens were placed in a ventilated environment after cleaned by running water. The SSRSW machine with high-frequency inverter power supply was produced by Miyachi Unitek Corporation. Flat tip electrode with 3.0 mm diameter was provided, and there was no cooling water during the welding process. Spot welds were made under the constant current mode. Electrode force (F), welding current (I) and welding time (T) were selected as the parameters to be optimized.

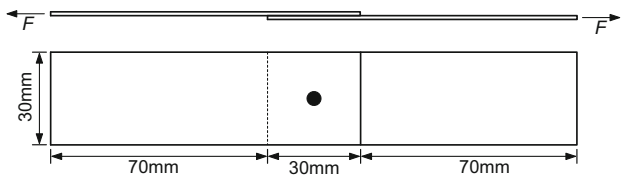

Fig. 1 Specimen dimensions for SSRSW

Static tensile-shear tests were carried out with an universal testing machine at constant cross-head speed of 1.0 mm/min. Failure load (F_l) and failure energy absorption (E) were used as quality characteristics. F_l referred to the peak value of load–displacement curve. E was the area under load–displacement curve up to F_l. Nugget diameter (D) was obtained by the vernier caliper at fractured faying surfaces. Spot-welded specimens were sectioned across the weld nugget for metallographic examination. After ground, polished and etched, optical microscope was utilized to detect the microstructure variation.

4 Results and Discussion

4.1 Microstructure Analysis

A typical microstructure variation in the spot weld is given in Fig. 2. Base metal, heat-affected zone and fusion zone are illustrated in Fig. 2b–d, respectively. The weld nugget boundary could be clearly identified in Fig. 2a. Directional and columnar grains growing from the fusion boundary toward weld center line are formed in fusion zone. Uniformly distributed fine α grain could be seen in base metal (Fig. 2b). Grain size in the heat-affected zone is coarser than base metal, which could be explained by the higher heat generation concentration. Needle-like martensite is formed in fusion zone (Fig. 2d), which is due to the high cooling rate after welding current is cut off.

4.2 Grey Relational Analysis (GRA)

Experiments are arranged as per the Taguchi's L9 orthogonal array design in GRA. The three factor levels selected

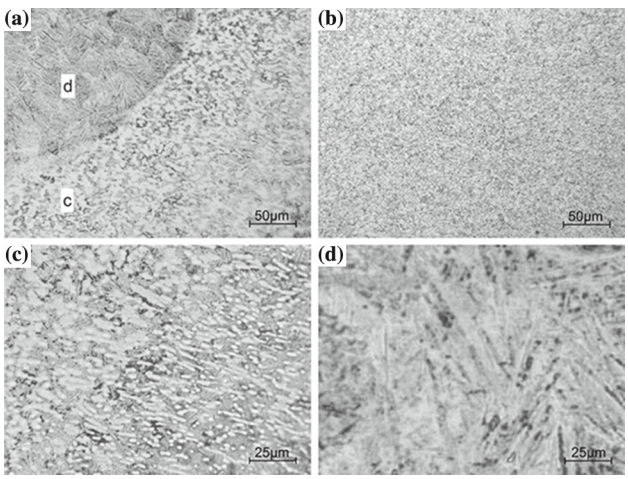

Fig. 2 Typical microstructure of small-scale resistance spot-welded TC2 titanium alloy

Table 2 Factor levels in Taguchi's L9 orthogonal array design

Welding parameter	Unit	Symbol	Level 1	Level 2	Level 3
Electrode force	N	F	75	125	175
Welding current	kA	I	1.0	1.6	2.2
Welding time	ms	T	4	8	12

are given in Table 2. Measured and normalized responses of nugget diameter, failure load and failure energy are depicted in Table 3. In order to determine the weight ω_i in grey relational grade calculation, PCA is made first on normalized responses, as listed in Table 4. Eigenvalues are aligned in descending order. As could be seen, the first principal component (PC_1) accounts for 94.8 % of total variance. The PC_1 alone is supposed enough to represent most information of original data, and could be adopted as the indicator of composite weld quality. Scores of the PC_1 are listed in Table 5. Rank of PC_1 implies that the spot weld under welding condition of experiment No. 9 possesses the best composite weld quality.

Grey relational coefficient ξ is derived from Eq. (4). The distinguishing coefficient ζ is defined as 0.5. The weight ω_i in Eq. (5) is determined by square value of corresponding component in eigenvector of PC_1. Weights are calculated as 0.3317, 0.3435 and 0.3249 for D, F_l and E, respectively. Evaluation of multiple quality characteristics by grey relational grade is given in Table 6. Grey relational grade is the largest at experiment No. 9, which is the same as that in PCA.

Response table is built to analyze average grey relational grade at each welding parameter level, as given in Table 7. The corresponding response graph for grey relational grade is depicted in Fig. 3, in which the overall average grey relational grade is represented by a dashed line. Maximum grey relational grade is at level 3 for all welding parameters. Optimum welding parameters combination could thus be established as $F_3I_3T_3$. Δ is the range between maximum and minimum grey relational grade for each welding parameter. Grey relational grade is varied the most with welding current ($\Delta = 0.4029$), followed by is the welding time ($\Delta = 0.2362$). Analysis of variance (ANOVA) for grey relational grade is given in Table 8. Percent contributions of welding current, welding time and electrode force are 65.17, 25.75 and 0.49 % respectively. Percent contribution generally indicates the welding parameter effect on grey relational grade. Welding current is thus suggested as the most influential parameter on quality characteristics. Effect of electrode force on weld quality is the least significant.

Both the PCA and GRA are proved useful in solving multi-objective optimization problem proposed here. However, optimum welding parameters determined by the orthogonal array design are just a rough estimation. Further analysis

Table 4 Principal component analysis (PCA)

Principal component	PC_1	PC_2^*	$PC_3^\dagger$
Eigenvalue (−)	2.8441	0.1233	0.0326
Proportion (%)	94.8	4.1	1.1
Cumulative (%)	94.8	98.9	100.0
Eigenvector	0.5759	−0.6217	−0.5309
	0.5861	−0.1388	0.7983
	0.5700	0.7708	−0.2844

PC_2^*, the second principal component
$PC_3^\dagger$, the third principal component

Table 5 Scores of the first principal component (PC_1)

No.	PC_1	Rank
1	0.0000	9
2	1.0303	5
3	1.6257	2
4	0.5778	7
5	1.3914	3
6	1.0470	4
7	0.5492	8
8	0.5955	6
9	1.6754	1

Table 3 Experimental data in Taguchi's L9 orthogonal array design

No.	Welding parameters			Measured responses			Normalized responses		
(−)	F (N)	I (kA)	T (ms)	D (mm)	F_l (N)	E (J)	D (−)	F_l (−)	E (−)
1	75	1.0	4	0.49	400.15	0.13	0.0000	0.0000	0.0000
2	75	1.6	8	1.63	2014.65	1.96	0.6994	0.6500	0.4326
3	75	2.2	12	2.12	2685.03	3.92	1.0000	0.9199	0.8960
4	125	1.0	8	1.22	1321.58	0.89	0.4479	0.3710	0.1797
5	125	1.6	12	1.91	2240.36	3.51	0.8712	0.7409	0.7991
6	125	2.2	4	1.68	1896.30	2.16	0.7301	0.6024	0.4799
7	175	1.0	12	1.37	1193.10	0.51	0.5399	0.3193	0.0898
8	175	1.6	4	1.28	1569.83	0.43	0.4847	0.4709	0.0709
9	175	2.2	8	1.96	2883.94	4.36	0.9018	1.0000	1.0000

Table 6 Grey relational analysis (GRA)

No.	Grey relational coefficients			GRG*	Rank
	D	F_l	*E*		
1	0.3333	0.3333	0.3333	0.3334	9
2	0.6245	0.5882	0.4684	0.5614	5
3	1.0000	0.8619	0.8278	0.8967	2
4	0.4752	0.4429	0.3787	0.4328	8
5	0.7952	0.6587	0.7134	0.7218	3
6	0.6494	0.5570	0.4901	0.5660	4
7	0.5208	0.4235	0.3546	0.4334	7
8	0.4925	0.4859	0.3499	0.4439	6
9	0.8358	1.0000	1.0000	0.9456	1

*GRG** grey relational grade

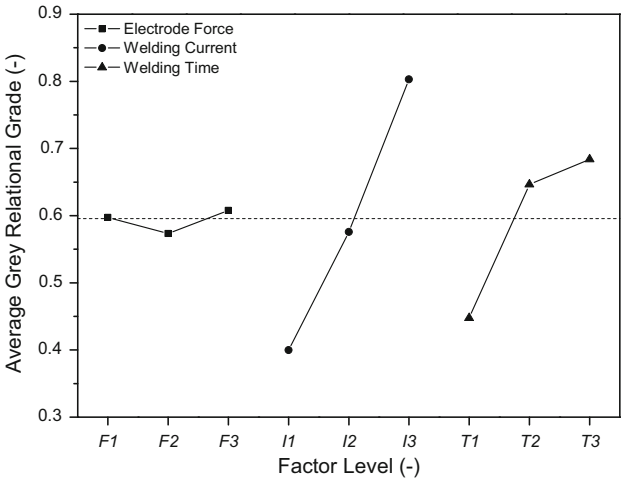

Fig. 3 The response graph for grey relational grade

is needed to establish the final optimum welding parameters combination.

4.3 Multiple Regression Analysis

4.3.1 Model Summary

The Box–Behnken experimental design is used for multiple regression analysis. Coded and actual factor levels are depicted in Table 9. Center point is repeated for five times. Center point is designed as the optimum welding parameter levels obtained in GRA. Measured multiple quality characteristics are given in Table 10. Backward regression method is used for nugget diameter prediction. Stepwise regression model is employed for failure load and failure energy estimation. In order to maintain similarity in appearance of regression equations between coded and actual units, all main effects presented in interaction terms are added into the model despite statistical significance on their own, which is called the hierarchy principle.

Failure energy is an important weld quality characteristic. Statistical model summary on failure energy is studied as a representative case. Model adequacy is evaluated through R^2 (=0.9373), adjust R^2 (=0.8746) and standard deviation (=0.40). R^2 and adjust R^2 are the larger the better. Standard deviation is the smaller the better. The model adequacy on failure energy prediction is found satisfactory as a whole. A scatter plot of predicted versus measured failure energy is shown in Fig. 4. Predicted failure energy could be found in good agreement with measured ones. ANOVA is established assuming that residuals are normally distributed with constant variance. Normal probability test of residuals is depicted in Fig. 5. Studentized residuals versus predicted failure energy is given in Fig. 6. As could be seen, the normal distribution and constant variance assumption of residuals are verified.

ANOVA is then performed to test statistical significance of the developed failure energy regression model, as given in Table 11. If P value is smaller than 0.05, it could be determined that the term influence on response is significant at 95 % confidence level. "Model F value" of 14.95 implies that the model is significant. There is only a 0.05 % chance that a "Model F value" this large could occur due to noise. P values of I, T, FI, IT terms are smaller than 0.05, which indicate that linear correlations of these terms with failure energy are obvious. Insignificant model terms like the F term are included following hierarchy principle. Five replicates at the center point are used to estimate pure error sum of squares. P value of the "*Lack of Fit*" term is 0.7935, which shows that the "*Lack of Fit*" term is not significant relative to pure error. There is a 79.35 % chance that a "*Lack of Fit F* value" this large could occur due to noise. Insignificant "*Lack of Fit*" term is desirable for the proposed model.

Table 7 The response table for grey relational grade

Welding parameter	Level 1	Level 2	Level 3	$\Delta^{\dagger}$	Rank
Electrode force	0.5972	0.5735	0.6076*	0.0341	3
Welding current	0.3999	0.5757	0.8028*	0.4029	1
Welding time	0.4478	0.6466	0.6840*	0.2362	2

Overall average grey relational grade = 0.5928
*, $Maximum$; $\Delta^{\dagger} = Maximum - Minimum$

Table 8 Analysis of variance (ANOVA) on grey relational grade

Source	Sum of squares	DF	Mean square	*F* value	*P* value	Contribution (%)
F	0.0018	2	0.0009	0.06	0.946	0.49
I	0.2448	2	0.1224	7.58	0.116	65.17
T	0.0967	2	0.0484	3.00	0.250	25.75
Error	0.0323	2	0.0161			8.59
Total	0.3756	8				100.00

Table 9 Factor levels in multiple regression analysis

Welding parameter	Unit	Symbol	Levels		
			−1	0	1
Electrode force	N	*F*	150	175	200
Welding current	kA	*I*	2.0	2.2	2.4
Welding time	ms	*T*	10	12	14

Table 10 The Box–Behnken experimental design

No.	Welding parameters			Measured responses		
(−)	*F* (N)	*I* (kA)	*T* (ms)	*D* (mm)	F_l (N)	*E* (J)
1	150	2.0	12	2.09	3323.98	4.13
2	200	2.0	12	2.12	3281.07	4.16
3	150	2.4	12	2.27	3316.29	5.22
4	200	2.4	12	2.35	3267.65	7.12
5	150	2.2	10	1.94	3027.82	4.60
6	200	2.2	10	2.09	2661.78	3.73
7	150	2.2	14	2.19	3330.60	5.57
8	200	2.2	14	2.01	3344.80	6.14
9	175	2.0	10	2.12	3030.34	4.22
10	175	2.4	10	2.23	3250.73	5.03
11	175	2.0	14	2.02	3409.04	3.70
12	175	2.4	14	1.98	3833.42	7.84
13	175	2.2	12	2.21	3260.35	5.25
14	175	2.2	12	2.18	3079.65	4.93
15	175	2.2	12	2.12	3184.62	4.63
16	175	2.2	12	2.29	3429.83	5.68
17	175	2.2	12	2.31	3347.28	5.74

4.3.2 Interaction Effect of Welding Parameters on Failure Energy

Response surface and contour plot of regression model should be analyzed for a comprehensive understanding of interaction effect. Influence of electrode force on weld quality has been proven the least significant in GRA. Interaction effect of welding parameters is thus emphasized on welding current and welding time, while the electrode force is kept constant at 200 N. The developed regression equation for failure energy prediction in coded factors is summarized as follows:

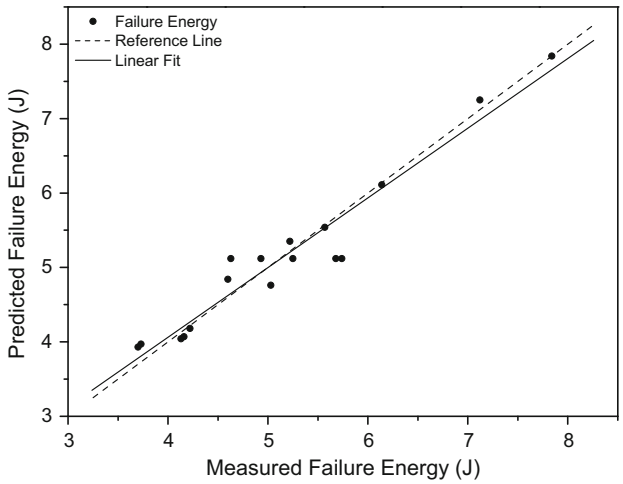

Fig. 4 Predicted versus measured failure energy in multiple regression analysis

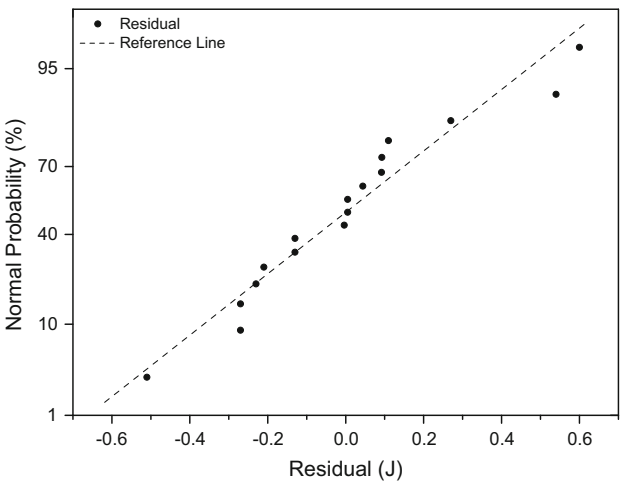

Fig. 5 Normal probability of residuals in failure energy regression model

$$E_{coded} = 5.14 - 0.075F + 1.13I + 0.71T + 0.47FI + 0.36FT + 0.83IT + 0.036I^2 + 0.56FI^2 \quad (6)$$

Effect of welding parameters on failure energy is depicted in Fig. 7. An overall increasing trend of failure energy with both parameters could be found. Failure energy is the minimum under $I = 2.0$ kA and $T = 10$ ms welding condition

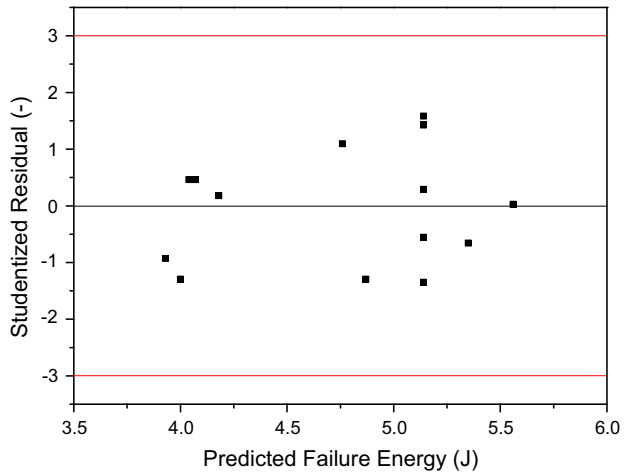

Fig. 6 Studentized residuals versus predicted failure energy in multiple regression analysis

owing to the smallest nugget diameter and failure load. Heat input increases with increasing welding current and welding time. More base material is melted, and the nugget diameter enlarges as a consequence. Cooling rate after welding increases and microstructure formed in the weld nugget gets hard, which could promote the load capacity of spot welds. When the welding current (or welding time) is held at high level, failure energy increases obviously with welding time (or welding current). This could be explained from the significant variation of heat input. Failure energy is the maximum under $I = 2.4\,\text{kA}$ and $T = 14\,\text{ms}$ welding condition.

4.3.3 Sensitivity Analysis for Failure Energy

Sensitivity analysis for failure energy depicts the increasing or decreasing tendency with small changes of welding parameter. It could be used to establish an effective weld quality control strategy. Sensitivity equations are designed as the partial derivative of failure energy with respect to electrode force, welding current and welding time, which are given in Eqs. (7), (8) and (9), respectively. The sensitivity analysis is carried out in Fig. 8. When one particular welding parameter is varied from −1 to 1, the other two welding parameters are kept constant at coded 0 level.

$$\frac{\partial E}{\partial F} = -0.075 + 0.47I + 0.36T + 0.56I^2 \tag{7}$$

$$\frac{\partial E}{\partial I} = 1.13 + 0.47F + 0.83T + 0.072I + 1.12FI \tag{8}$$

$$\frac{\partial E}{\partial T} = 0.71 + 0.36F + 0.83I \tag{9}$$

Analysis on electrode force sensitivity is shown in Fig. 8a. Electrode force sensitivity is mostly negative, which indicates a decrease in failure energy with the increase in electrode force regardless of welding parameter level. Actually, heat input is reduced as electrode force increases due to the dynamic resistance reduction. Failure energy of a spot weld is closely related to the heat input. Electrode force sensitivity is increased significantly as welding current varies from 0 to 1, which implies that failure energy is sensitive to electrode force variation under high welding current condition. Effect of welding time on electrode force sensitivity is also significant. When welding time is increased from −1 to 1, electrode force sensitivity varies obviously from negative to positive. Expulsion is easy to occur under high welding current or long welding time condition. A larger electrode force is beneficial for expulsion prevention, by which the weld quality could be improved.

All welding current sensitivity values are positive under different welding conditions, as shown in Fig. 8b. Failure energy increases with welding current increasing despite the welding parameter level. The welding current sensitivity is

Table 11 Analysis of variance (ANOVA) on the developed failure energy regression model

Source	Sum of squares	DF	Mean square	*F* value	*P* value
Model	19.2678	8	2.4085	14.9542	0.0005
F	0.0225	1	0.0225	0.1397	0.7183
I	10.1250	1	10.1250	62.8662	<0.0001
T	4.0186	1	4.0186	24.9516	0.0011
FI	0.8742	1	0.8742	5.4281	0.0482
FT	0.5184	1	0.5184	3.2187	0.1105
IT	2.7722	1	2.7722	17.2128	0.0032
I^2	0.0056	1	0.0056	0.0348	0.8566
FI^2	0.6216	1	0.6216	3.8596	0.0851
Residual	1.2885	8	0.1611		
Lack of fit	0.3767	4	0.0942	0.4132	0.7935
Pure error	0.9117	4	0.2279		
Cor total	20.5562	16			

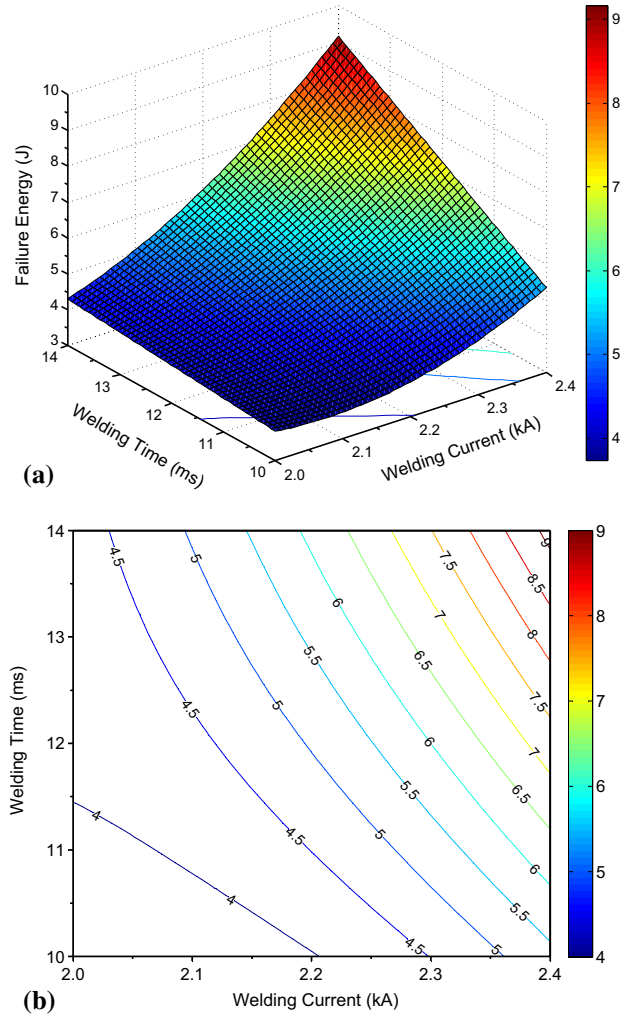

Fig. 7 Interaction effect of welding parameters on failure energy in multiple regression analysis ($F = 200\,\mathrm{N}$). **a** Response surface plot. **b** Contour plot

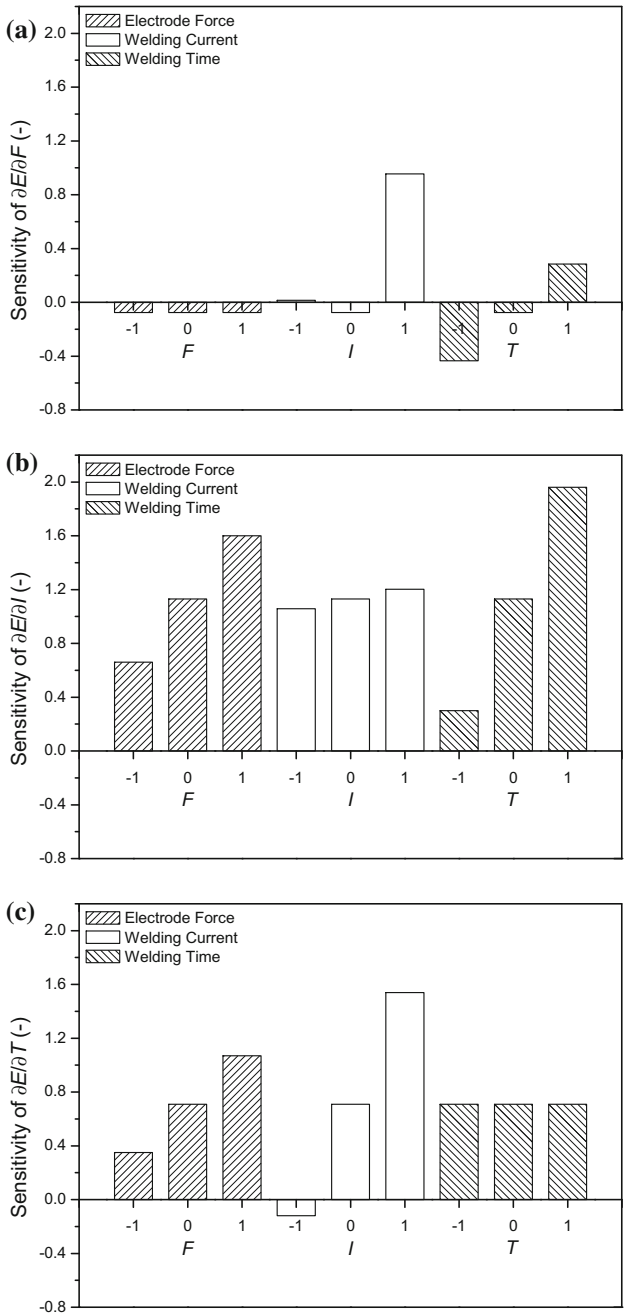

Fig. 8 Sensitivity analysis on developed failure energy regression model. **a** Electrode force sensitivity. **b** Welding current sensitivity. **c** Welding time sensitivity

also increased with welding parameter. Figure 8c shows the welding time sensitivity analysis, in which the sensitivity values are mostly positive. That is to say, failure energy increases consistently with welding time under different welding parameters combination conditions. Welding parameter sensitivity could be ranked as follows: $I > T > F$, referring to the average sensitivity value. Welding current is found the most influential parameter on weld quality improvement.

4.3.4 Optimizing Welding Parameters

Optimum welding parameters are first determined by desirability function approach. Each response is converted into a desirability value g_i between 0 and 1 by the corresponding criterion. An ideal response value is represented by $g_i = 1$. The overall desirability G is defined as:

$$G = (g_1 \times g_2 \times \cdots \times g_k)^{1/k} \tag{10}$$

where k is the number of quality characteristics. Then the optimization strategy is transformed into searching welding parameters under which condition the overall desirability is the maximum. Desirability is the largest when $F = 200\,\mathrm{N}$, $I = 2.4\,\mathrm{kA}$ and $T = 14\,\mathrm{ms}$, the predicted nugget diameter,

Table 12 Multi-objective genetic algorithm approach

No.	Welding parameters			Measured responses		
(−)	F (N)	I (kA)	T (ms)	D (mm)	F_l (N)	E (J)
1	199.9075	2.3998	13.9881	2.1472	3652.1013	9.1342
2	167.6850	2.4000	13.9972	2.0480	3841.0880	7.4584
3	150.1775	2.3985	13.4661	2.2956	3627.7746	6.2253
4	150.3225	2.3980	13.7595	2.2775	3699.7273	6.4044
5	150.7600	2.3993	13.9079	2.2603	3744.7932	6.5171
6	199.9450	2.3997	13.9490	2.1538	3640.7954	9.0967
7	199.8675	2.3997	12.1236	2.3244	3256.2882	7.3601
8	150.2350	2.3950	13.5722	2.2883	3645.5619	6.2853
9	200.0000	2.3998	11.7271	2.3312	3198.3515	6.9903
10	155.8775	2.3995	13.9055	2.1828	3778.3177	6.7801

failure load and failure energy are 2.15 mm, 3654.7 N and 9.15 J respectively.

Multiple responses in desirability function approach must be converted into the overall desirability. In order to obtain optimum welding parameters combination directly, the genetic algorithm is applied as well. Genetic algorithm is based on the mechanics of biological evolution process [14]. Individuals with higher fitness possess a larger chance to survive and produce higher fitness offspring. Genetic algorithm starts with the initial population which is randomly formed. Solution space is well explored using the initial population of individuals. Then fitness values of all individuals are evaluated. Individuals are operated by selection, crossover and mutation at each iteration. The population is modified repeatedly until a stopping criterion is satisfied or an optima is reached. It is very different from traditional optimization methods. The simplicity, easy operation and global perspective of genetic algorithm have been validated.

Multi-objective genetic algorithm is adopted here. The concept of Pareto optimal set is used. A Pareto optimal solution x_1 is defined as:

$$f_i(x_1) \leqslant f_i(x_2), \forall i \in 1, 2, \ldots, p. \tag{11}$$

$$f_j(x_1) \leqslant f_j(x_2), \exists j \in 1, 2, \ldots, p. \tag{12}$$

where p is the number of objective functions f to be minimized. A series of these optimal solutions make up the Pareto optimal set. Corresponding objective function values are called the Pareto front.

The first ten Pareto optimal solutions and Pareto front are listed in Table 12. Considering the limited variation of nugget diameter, optimum welding parameters could be determined by a best combination of failure load and failure energy. Therefore the No. 1 welding condition is more preferred than others, which is in accordance with desirability function approach.

4.4 Back Propagation Neural Network (BPNN) Analysis

Neural network is cost-effective, easy to understand and has been employed in the manufacturing process. BPNN is one of the well-known supervised learning neural network models. It has a multilayer feed-forward structure (error back propagation algorithm) with input, hidden and output layers. In this section, MATLAB neural network toolbox is utilized to build the BPNN. Experimental data from the GRA and multiple regression analysis are adopted. Input parameters of BPNN are selected as the electrode force, welding current and welding time. PCA is conducted on measured responses of nugget diameter, failure load and failure energy. PC_1 is adopted as the composite weld quality indicator. The output of BPNN is designed as scores of the PC_1. Among the 22 experimental results, a randomly selected seventeen input–output data are used to train the network, and the remaining five groups of data are prepared for testing.

Determination of the network architecture is an important task in BPNN analysis. There is no strict criterion in selecting the number of hidden layers and neurons in each hidden layer. Purelin transfer function is applied as the activation function for hidden and output layers. Levenberg–Marquardt algorithm is used for network training. The structure is finally determined as 3–6–1 after various trial and error attempts. The relationship between inputs and outputs could thus be constructed. Predicted versus actual values for the PC_1 is shown in Fig. 9. Data for training are illustrated as solid circles, and data for testing are given as open circles. As could be seen, linear fit is very close to the reference line. Performance of the developed neural network model is satisfactory. After training and testing, optimization of the weld quality indicator PC_1 is realized by genetic algorithm and particle swarm optimization.

Particle swarm optimization is a population-based stochastic technique inspired by social behavior of bird flocking,

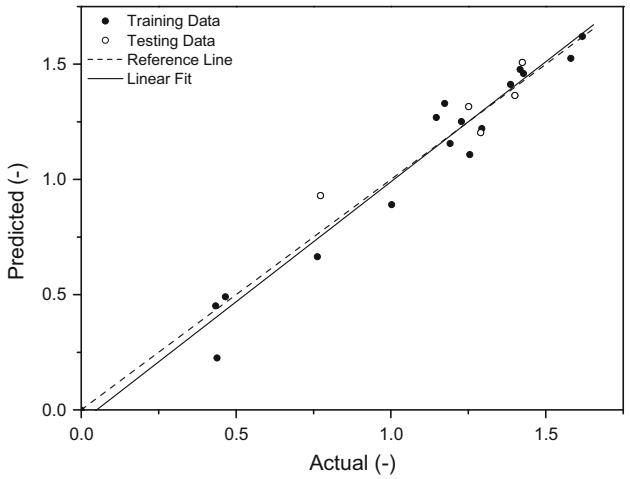

Fig. 9 Predicted versus actual values for PC_1 by the proposed neural network model

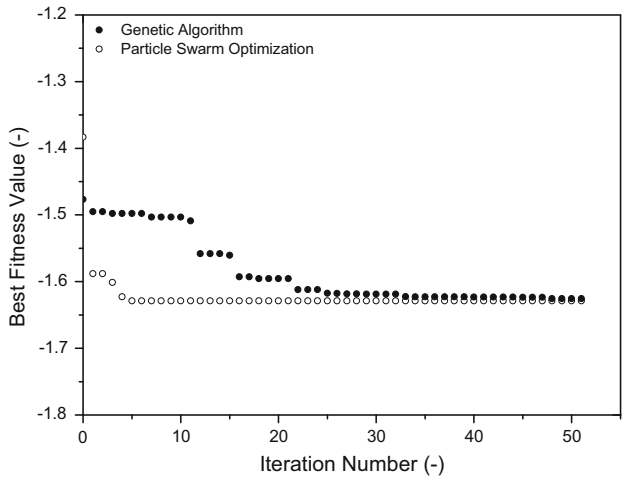

Fig. 10 The best fitness value variation with iteration number in neural network analysis

which was developed by Kennedy and Eberhart [15]. The population behaves like birds collectively looking for prey. Particles explore the solution space through following current optimum ones. Each particle moves with a certain velocity toward the best position in one iteration. Many similar features are existed between particle swarm optimization and genetic algorithm. A randomly initialized population are both used to search for the optima through updating generations. Unlike genetic algorithm, no evolution operators are adopted in particle swarm optimization. There are few parameters to adjust in particle swarm optimization. Particle swarm optimization has been successfully applied in a wide range of fields.

Fitness function value is defined as the opposite value of PC_1. This is due to the fact that PC_1 is the larger the better, but optimization methods are used to search the smallest value of fitness function. The population size is set as twenty. The stopping criterion on iteration number is 100 for both methods. The selection, crossover and mutation function in genetic algorithm are used as "stochastic uniform," "scattered" and "constraint dependent," respectively. The factor of acceleration in particle swarm optimization is set as 1.49. Variation of the best fitness value with iteration number is shown in Fig. 10. As could be found, best fitness values are rapidly converged to the optima. Performance of the particle swarm optimization is obviously better than genetic algorithm. The finally established optimum welding parameters combination is: $F = 200\,\text{N}$, $I = 2.4\,\text{kA}$ and $T = 14\,\text{ms}$.

4.5 Confirmation Experiment

Optimum welding parameters obtained from GRA, multiple regression analysis and BPNN are listed in Table 13. An identical optimum design could be obtained in multiple regression and BPNN analysis separately. The neural network model is found more effective in searching global optimum solution directly. After obtaining optimum welding parameters, the next step is to verify improvement on quality characteristics. As depicted in Table 13, experimental results of nugget diameter, failure load and failure energy are obviously better than those in Table 3 and Table 10. In addition, a good agreement in quality characteristics could be found between regression based estimation in Table 12 (No. 1) and confirmation experiment in Table 13. The proposed methods are proved effective in simultaneous optimization of multiple quality characteristics in SSRSW of titanium alloy.

5 Conclusions

In this study, the GRA, multiple regression analysis and BPNN were applied to predict and optimize multiple quality characteristics in titanium alloy SSRSW. A rough estimation of optimum welding parameters was first given through

Table 13 Results of confirmation experiment

Method	Optimum design			Measured responses		
(−)	F (N)	I (kA)	T (ms)	D (mm)	F_l (N)	E (J)
GRA	175	2.2	12	2.23	3258.42	5.20
Regression analysis	200	2.4	14	2.34	3594.16	9.28
BPNN	200	2.4	14			

GRA. Welding current was found the most significant parameter affecting quality characteristics. An experimental design for multiple regression analysis was then made based on the GRA. Interaction effect of welding parameters on failure energy was analyzed. Sensitivity analysis for failure energy was implemented as well. Desirability function approach and multi-objective genetic algorithm were utilized to establish the optimum welding parameters. A BPNN model was also performed to search the global optimum welding parameters directly. The PC_1 was used as the composite weld quality index. Particle swarm optimization was found more effective in adopting the optimum welding parameters combination than genetic algorithm. Experimental results showed that quality characteristics were significantly improved. The neural network-based model was found better than multiple regression analysis in directly searching global optimum welding parameters combination.

Acknowledgments We are grateful to the financial support from the National Natural Science Foundation of China (Grant No. 11072083) and the Doctoral Dissertation Innovation Fund of Huazhong University of Science and Technology (Grant No. 0118240059). The authors would like to thank Zongguo Lin and Suning Sheng from Miyachi Unitek Corporation for providing the welding machine. Experimental support from the Analysis and Testing Centre of Huazhong University of Science and Technology is also acknowledged.

References

1. Dalgaard, E.; Wanjara, P.; Gholipour, J.; Cao, X.; Jonas, J.J.: Linear friction welding of a near-β titanium alloy. Acta Mater. **28**(2), 770–780 (2012)
2. Kahraman, N.: The influence of welding parameters on the joint strength of resistance spot-welded titanium sheets. Mater. Des. **28**(2), 420–427 (2007)
3. Wan, X.; Wang, Y.; Zhao, D.: Quality monitoring based on dynamic resistance and principal component analysis in small scale resistance spot welding process. Int. J. Adv. Manuf. Technol. (2016). doi:10.1007/s00170-016-8374-1
4. Ely, K.J.; Zhou, Y.: Microresistance spot welding of Kovar, steel, and nickel. Sci. Technol. Weld. Join. **6**(2), 63–72 (2001)
5. Kesharwani, R.K.; Panda, S.K.; Pal, S.K.: Multi objective optimization of friction stir welding parameters for joining of two dissimilar thin aluminum sheets. Procedia Mater. Sci. **6**, 178–187 (2014)
6. Gupta, S.K.; Pandey, K.N.; Kumar, R.: Multi-objective optimization of friction stir welding of aluminium alloy using grey relation analysis with entropy measurement method. Nirma Univ. J. Eng. Technol. **3**(1), 29–34 (2015)
7. Korra, N.N.; Vasudevan, M.; Balasubramanian, K.R.: Multi-objective optimization of activated tungsten inert gas welding of duplex stainless steel using response surface methodology. Int. J. Adv. Manuf. Technol. **77**(1-4), 67–81 (2015)
8. Saurav, D.; Goutam, N.; Asish, B.; Pradip, K.P.: Application of PCA-based hybrid Taguchi method for correlated multi criteria optimization of submerged arc weld: a case study. Int. J. Adv. Manuf. Technol. **45**, 276–286 (2009)
9. Tiwary, A.P.; Pradhan, B.B.; Bhattacharyya, B.: Parametric optimization of micro-EDM process using response surface methodology and principal component analysis. J. Manuf. Technol. Res. **5**(3/4), 117–136 (2013)
10. Muhammad, N.; Manurung, Y.H.; Jaafar, R.; Abas, S.K.; Tham, G.; Haruman, E.: Model development for quality features of resistance spot welding using multi-objective Taguchi method and response surface methodology. J. Intell. Manuf. **24**(6), 1175–1183 (2013)
11. Shojaeefard, M.H.; Behnagh, R.A.; Akbari, M.; Givi, M.K.B.; Farhani, F.: Modelling and Pareto optimization of mechanical properties of friction stir welded AA7075/AA5083 butt joints using neural network and particle swarm algorithm. Mater. Des. **44**, 190–198 (2013)
12. Pashazadeh, H.; Gheisari, Y.; Hamedi, M.: Statistical modeling and optimization of resistance spot welding process parameters using neural networks and multi-objective genetic algorithm. J. Intell. Manuf. (2014). 10.1007/s10845-014-0891-x
13. Deng, J.: Control problems of grey systems. Syst. Control Lett. **5**, 288–294 (1982)
14. Holland, J.: Adaptation in Natural and Artificial System. University of Michigan Press, Ann Arbor (1975)
15. Kennedy, J.; Eberhart, R.: Particle swarm optimization. In: Proceedings of the IEEE International Conference on Neural Networks, Perth, Australia, pp. 1942–1948 (1995)